

Use of WorldView-2 stereo imagery and National Forest Inventory data for wall-to-wall mapping of growing stock



Markus Immitzer ^{a,*}, Christoph Stepper ^b, Sebastian Böck ^a, Christoph Straub ^b, Clement Atzberger ^a

^aInstitute of Surveying, Remote Sensing and Land Information (IVFL), University of Natural Resources and Life Sciences, Vienna (BOKU), Peter-Jordan-Straße 82, A-1190 Vienna, Austria

^bBavarian State Institute of Forestry (LWF), Department of Information Technology, Research Group: Remote Sensing, Hans-Carl-von-Carlowitz-Platz 1, D-85354 Freising, Germany

ARTICLE INFO

Article history:

Received 21 July 2015

Received in revised form 8 October 2015

Accepted 10 October 2015

Keywords:

Angle-count sampling

Feature selection

Forest inventory

Random Forests

Remote sensing

ABSTRACT

Angle-count sampling (ACS) is an established method in forest mensuration and is implemented in different National Forest Inventories (NFI). However, due to the lack of fixed reference areas of the inventory plots, these ACS-based field data are seldom used as training data for wall-to-wall mapping applications at forest enterprise level. In this paper, we demonstrate an approach to overcome this shortcoming. For a study area in northern Bavaria, Germany, we used ACS-based NFI data for model training to generate wall-to-wall maps of growing stock for broadleaf, conifer and mixed forest stands. Both spectral and height information from the very high resolution WorldView-2 (WV2) satellite were used as auxiliary information and the non-parametric Random Forests (RF) algorithm was chosen as modeling approach. The growing stock predictions were validated using out-of-bag (OOB) samples and further verified at the plot and stand level using additional data. For validation, field plots from a Management Forest Inventory (MFI) and delineated forest stands were used. Compared to stand-level aggregations based on field plots from the MFI, our approach explained 56% of the variability in the growing stock (R^2) with a relative RMSE of 15% at the stand level ($n = 252$). As expected, the scatter was higher at the plot-level ($n = 3973$). Nonetheless, the models still achieved acceptable performance measures ($R^2 = 0.44$; RMSE = 34%).

© 2015 Elsevier B.V. All rights reserved.

1. Introduction

Detailed, reliable and up-to-date information is essential for optimum management of forests. For example, structural descriptions of forests such as growing stock are required for mid-term forest management. Usually, the required information is obtained from terrestrial sample-based forest inventories. Several studies have demonstrated that the combination of terrestrial inventories with remote sensing further increases the value of terrestrial approaches such as supporting national forest inventories (e.g. McRoberts et al., 2014a; McRoberts and Tomppo, 2007). Remote sensing techniques can provide useful information over large areas, at reasonable costs, with short repetition intervals and with a higher level of detail (Masek et al., 2015; McRoberts et al., 2014c; Stoffels et al., 2015; Wulder and Franklin, 2003). This is of great interest for forest management applications (Næsset, 2014)

and for ecological purposes (Wulder et al., 2004; Zlinszky et al., 2015). In combination with inventory data remote sensing data can be used for stratification purposes (McRoberts et al., 2002; Tomppo et al., 2008), small area estimations (e.g. Breidenbach and Astrup, 2012; Steinmann et al., 2013) and to describe direct relationships between the two data sets (e.g. Stepper et al., 2015a).

For the mapping of structural forest variables such as spatial distribution of growing stock, a variety of different passive and active remote sensing sensors have been tested. Some studies used spectral information from (passive) satellite imagery such as Landsat or MODIS to model growing stock over large areas (e.g. Chirici et al., 2008; Falkowski et al., 2009; Gallau et al., 2010; Koukal et al., 2007; Reese et al., 2002). In some North European countries, the combination of satellite imagery and NFI data is already used to produce nationwide forest cover maps (Tomppo et al., 2008).

Although the availability of (active) airborne laser scanning (ALS) data over the past ten years has been increasing, however, the use of 3D data became more prominent due to its very high level of derived structural detail. The strength of ALS data is related to the three-dimensional forest structure information that it provides, along with the measurements of the terrain underneath.

* Corresponding author.

E-mail addresses: markus.immitzer@boku.ac.at (M. Immitzer), Christoph.Stepper@lwf.bayern.de (C. Stepper), sebastian.boeck@boku.ac.at (S. Böck), Christoph.Straub@lwf.bayern.de (C. Straub), clement.atzberger@boku.ac.at (C. Atzberger).

For this reason, ALS is often considered as one of the most promising remote sensing techniques for forest inventories (Vauhkonen et al., 2014). Recent and comprehensive reviews of ALS applications in forestry are provided by Wulder et al. (2012) and Maltamo et al. (2014). Operational applications of ALS for forest inventories have been reported for Norway (Næsset, 2007), Canada (Woods et al., 2011) and Finland (Maltamo et al., 2011). For the mentioned operational applications the area-based approach was used, as described in Næsset (2002, 2014) and White et al. (2013). In some cases, aerial images are used together with ALS to improve the separation of tree species (e.g. in Finland) (Maltamo et al., 2006).

Despite the known advantages of ALS, it is rarely used in practical applications. Due to relatively high acquisition costs, ALS data are not affordable as a data source for many countries, for regularly updating the forest description and for prediction of forest attributes. To cope with this problem, image matching techniques may be an alternative. Image matching allows the extraction of digital surface models (DSMs) from (air- and space-borne) stereo imagery and is therefore considered an interesting alternative to ALS-derived DSMs (White et al., 2013b). With adequate methods, and the availability of mostly ALS-based digital terrain models (DTM), image-based DSMs achieve sufficient precision for forest canopy height modeling (Hobi and Ginzler, 2012).

Advantages of airborne stereo data include lower acquisition costs and high repetition rate (Pitt et al., 2014; Rahlf et al., 2014; Stepper et al., 2015a; Straub et al., 2013a). Using stereo imagery, it is possible to combine the height information with spectral information to improve model accuracies (Maltamo et al., 2009). Recently, it has been demonstrated that the large side overlap of airborne imagery can be used to extract additional structural variables from the recorded directional variation of canopy reflectance (Koukal et al., 2014).

Recent studies used point clouds and canopy height models (CHM) derived from aerial images to predict growing stock at the plot and stand level (e.g. Rahlf et al., 2014; Stepper et al., 2015a). Other studies have assessed height changes based on regularly acquired aerial images (Stepper et al., 2015b; Vastaranta et al., 2015; Wang et al., 2015). The changes in the forest canopy height can be used to derive yield classes (Windisch et al., 2014) or age classes (Vastaranta et al., 2015) of the forests. The comparison of height data derived from ALS to those from aerial images revealed only slight differences in the prediction of forest inventory attributes. Studies were conducted for different forest types e.g. boreal forests in Finland (Gobakken et al., 2015; Nurminen et al., 2013; Vastaranta et al., 2013), conifer-dominated forests in Canada (Pitt et al., 2014) and mixed forests in Central Europe (Stepper et al., 2015a). All mentioned studies emphasize the great potential of aerial stereo imagery to support forest inventories if a pre-existing ALS-based DTM is available to normalize the photogrammetric measurements (i.e. for vegetation height calculation). Compared with ALS, the costs for acquiring aerial images are considerably lower, aerial images cost about one-half to one-third of ALS data (White et al., 2013b).

Thus far, few studies have used canopy height information obtained from very high-resolution (VHR) satellite stereo imagery for predictions of forest inventory attributes. St-Onge et al. (2008) assessed the accuracy of forest height and aboveground biomass estimations based on an Ikonos stereo pair and an ALS DTM in a study site located in Quebec, Canada. Straub et al. (2013b) used Cartosat-1 and WorldView-2 (WV2) stereo imagery for area-based predictions of growing stock in a highly structured mixed forest in Germany. Kattenborn et al. (2015) evaluated predictors from interferometric (Tandem-X) and photogrammetric (WV2) height models in combination with hyperspectral (EO1-hyperion) predictors for biomass estimations in a study site with both pure

and mixed stands in Germany. The main advantages of satellite data over airborne remote sensing data include higher temporal resolution, wider area coverage and spatially more homogenous image content. Additionally, satellites often have an improved spectral resolution (e.g. more and narrower bands) compared to state-of-the-art digital photogrammetric cameras.

There are two main approaches to estimate growing stock from 3D remote sensing data: single tree approach and area-based approach. In the single tree approach, remote sensing data are divided into segments representing single tree crowns. ALS data with very high point densities are required to model these single trees. The area-based approach is based on the statistical dependency between predictor variables derived from remote sensing data and field measured response variables, to infer from sample plots to large areas (e.g. Hollaus et al., 2009; Næsset, 2002; McRoberts et al., 2014b; Stepper et al., 2015a; White et al., 2013a).

In terms of statistical methods, both parametric regressions (e.g. Hollaus et al., 2009; Næsset, 2002; Maselli et al., 2014) as well as non-parametric methods have proved suitable for modeling growing stock. In the non-parametric domain, *k*-NN is amongst the most often chosen techniques, especially in applications dealing with NFI data and satellite images (e.g. Chirici et al., 2012; McRoberts et al., 2015; Tomppo et al., 2008). The successful use of Random Forests (RF) as an alternative non-parametric technique was demonstrated in several recent studies (e.g. Nurminen et al., 2013; Stepper et al., 2015a). Advantages of RF for that kind of application with numerous co-variates are the ease of feature reduction based on variable importance measures, the good performance in situations where many more predictors exist than samples ("large P, small N" situations), and the ability to use variables with different scales as predictors (White et al., 2013a).

One challenge in combining terrestrial forest inventories with remotely sensed data relates to the sampling design of the terrestrial inventories. For example, in many European countries, such as Germany, terrestrial forest inventories are conducted at different geographical scales. Local (small-scale) forest inventories provide information for specific forest holdings and are usually conducted in forests with a minimum size of around 50–100 ha. At the other end of the scale, national forest inventories provide large-scale information on forest condition and productivity (Kändler, 2006). However, the sample plots are usually widely spread, e.g. in Germany on a nationwide 4 km × 4 km grid (BMEL, 2015). In Europe, this information is generally updated every five to ten years (Tomppo et al., 2010).

To the best of our knowledge, studies in Central Europe dealing with wall-to-wall estimations based on 3D remote sensing data have used field plots from local inventories and not from large-scale NFI. One explanation as to why NFI samples are underused relates to the unresolved issue of spatially connecting the angle-count samples with the remote sensing data. Indeed, national inventories in Central Europe often use the angle-count approach where the inclusion probability of a tree is proportional to its basal area at breast height and to its distance to the plot center (Tomppo et al., 2010). For an individual tree, the covered ground area on a plot is a circle (if the diameter is assumed to be a circle) but not any more when merging the individual circles. However, well-specified reference areas would be preferred to build transfer relations between the field sample and the remote sensing data. A common way to deal with this challenge is to extract the remotely sensed information from a range of different plot sizes (circles) and evaluate their predictive power in subsequent modeling of the response variable e.g. the growing stock. The circle size with the best model performance is then identified and further used for wall-to-wall mapping. This implies that only one plot size is used (e.g. Hollaus et al., 2009; Immitzer, 2013). However, the selection of only one plot size will cause disadvantages: reference areas that

are too small may exclude some important remote sensing information whereas reference areas too large may be influenced by their neighborhood conditions. Additionally, the area covered by trees (crowns) in angle-count approaches seldom corresponds to a perfect circle. The degree of misalignment between the trees sampled in the field and the approximated circle used for extracting the remote sensing data depends on the stand characteristics.

The present study assesses the potential of very high resolution WV2 stereo data for an area-based prediction of growing stock in a broadleaf-dominated forest using existing field plots from the German NFI as training samples. For this purpose, a novel approach was developed to link the angle-count samples from the NFI with the remotely sensed spectral and CHM data. To evaluate the informative value of the predicted growing stock on the forest enterprise level, the predictions were validated at the plot and at the stand level using an MFI data set. WV2 was chosen for the study as this sensor offers data with a very high spatial resolution in eight spectral bands. These satellite data have already demonstrated a high suitability for classification applications in forests (Immitzer et al., 2012a,b; Immitzer and Atzberger, 2014; Omer et al., 2015; Waser et al., 2014).

The main objectives of the study are:

- modeling growing stock ($\text{m}^3 \text{ ha}^{-1}$) using (angle-count) NFI field data by implementing a novel multi-circle and multi-metrics approach,
- evaluating the explanatory power of spectral and height-related metrics for modeling growing stock, and
- developing a wall-to-wall application of the growing stock model by using a moving window approach.

2. Study area and materials

2.1. Study area

The study is centered in the *Steigerwald* test site ($49^\circ 55' \text{N}$, $10^\circ 35' \text{E}$) located in the northwestern part of Bavaria, Germany (Fig. 1). The study area encompasses a total area of 700 km^2 with elevations ranging from 210 m to 490 m above sea level (average 335 m a.s.l.). Soils are predominantly built up from Upper Triassic sandstone layers and the main land cover type within the study area is forested land (370 km^2). Thereof, 164 km^2 (44%) are state-owned land, which can be characterized as managed forest, with a great variety of stand development stages (Mergner, 2013). The main tree species in the area are European beech (*Fagus sylvatica* L., 42%), sessile oak (*Quercus petraea* (Mattuschka) Liebl., 18%) and Scots pine (*Pinus sylvestris* L., 14%).

2.2. Field data

2.2.1. National Forest Inventory data

The National Forest Inventory (NFI) in Germany, established in 1986, is based on a single-level cluster sampling and was reevaluated for the second time in 2012 (third inventory measurements – BWI³). The layout of the individual clusters, comprising four measurement plots located on a square (called 'tract') with a side length of 150 m, is based on a nationwide, permanent $4 \text{ km} \times 4 \text{ km}$ grid. All plots are examined for the current land cover type according to the German NFI definition (key requirements for forest: minimum area $\geq 0.1 \text{ ha}$, minimum width $\geq 10 \text{ m}$; for details refer to Polley et al. (2010)) and in consequence, only forested plots are surveyed in the field, i.e. clusters with less than four plots can exist. At each plot, more than 150 features are recorded using standardized techniques (BMEL, 2015; BMELV, 2011).

In contrast to inventory designs using fixed area plots, the German NFI is based on the angle-count sampling (ACS;

Bitterlich, 1948). The inclusion probability of a tree is proportional to its basal area at defined height; therefore each tree trunk is focused from the sample plot center and is selected if the diameter at breast height (dbh) exceeds a prescribed angle width. Within the German NFI, a basal area factor of four is used, i.e. each sample tree represents a basal area of $4 \text{ m}^2 \text{ ha}^{-1}$. For volume estimation, all trees selected by ACS with dbh $\geq 7 \text{ cm}$ are callipered and tree heights are measured for a sub-sample. Heights of the remaining trees are predicted using established diameter-height-models and taper curves are applied to obtain individual tree volumes. Subsequently, these individual tree volumes are converted to per hectare values (Laar and Akça, 2007) and aggregated for the respective plots. According to Polley et al. (2010), the growing stock estimates used in the current study refer to volume (m^3) of compact wood, i.e. above-ground stem volume including bark having a diameter of at least 7 cm.

Within the presented study area (Fig. 1), a total of 92 sample plots (tract corners) were assigned to be forest following the NFI definition (BMELV, 2011). The field measurements were conducted in the years 2011 and 2012 and a Cosifan-MCC1 GNSS device was used to record the respective plot centers, achieving accuracies with maximum deviations of 3 m under closed canopies (H. Klemmt, personal communication, 18 May 2015). Field based estimates of growing stock, separately for conifers and broad-leaves, were made available for the 92 NFI sample plots.

2.2.2. Management Forest Inventory

To further validate the modeling results, field measurements from a Management Forest Inventory (MFI) were used as a separate validation data set. These MFI data were acquired in 2010 by the Bavarian State Forest Enterprise (BaySF). The guideline of BaySF (2011) provides a basic description of the methodology, further details regarding the inventory design are given e.g. in Straub et al. (2013a). The permanent field plots, fixed circles with an area of 500 m^2 , are laid out in a regular grid pattern of $200 \text{ m} \times 200 \text{ m}$ within the state-owned land (cf. Fig. 1). For all plots, the location of the center point was measured using a Trimble GeoExplorer XT GPS device with maximum deviations of $\pm 3\text{--}5 \text{ m}$ (H. Grünvogel, personal communication, 4 August 2014). In total, measurements for 3937 MFI plots were recorded within the study area and were made available to us. For all plots, per-hectare values for various forest-related attributes, e.g. growing stock, from the individual tree data were compiled. Descriptive statistics for both the NFI and MFI field data are shown in Table 1.

2.2.3. Operational management units

In addition to the model validation at the plot level, the model predictions were compared to stand level estimates. For this purpose, MFI plot measurements were aggregated for separate operational management units (forest stands). The stand delineation of the state-owned forest was carried out manually by forest-management professionals based on CIR orthophoto (GSD 20 cm) interpretation and field surveys in 2012 in accordance with BaySF (2011). Here, characteristics such as tree species composition, developmental stage and vertical, as well as horizontal stand structures were considered. In total, 2330 stands, varying in size from 1 to 9 ha (avg. size 7 ha), were established within the state-owned land. These geometries were intersected with the MFI inventory plot locations and following Stepper et al. (2015a), we selected only forest stands which contained at least five sample plots for the assessment of the growing stock prediction at the stand level. In total 252 stands with an average size of 29.2 ha (SD: 11.6 ha) remained for this purpose. The observed growing stock, derived as the mean of the terrestrial inventory plots, ranged from 73.0 to $637.7 \text{ m}^3 \text{ ha}^{-1}$ with an arithmetic mean of $390.6 \text{ m}^3 \text{ ha}^{-1}$ (SD: $84.9 \text{ m}^3 \text{ ha}^{-1}$).

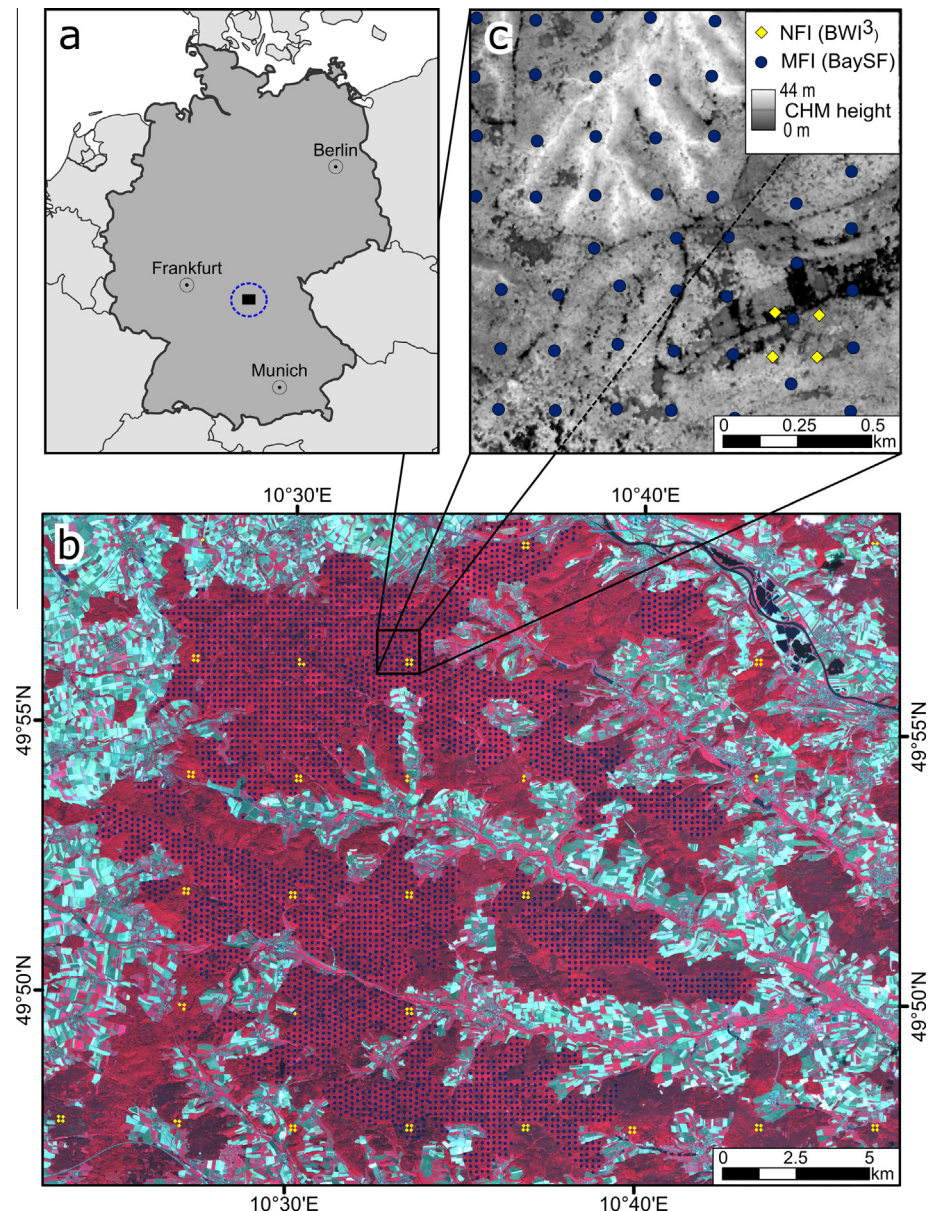


Fig. 1. Map of the study area. (a) Location in Germany, (b) spatial distribution of the full set of ground plots (yellow: National Forest Inventory (NFI) plots, blue: Management Forest Inventory (MFI) plots) superimposed on a CIR composite of a WorldView-2 image, and (c) detailed map illustrating the image-based CHM and the spatial arrangement of the inventory plots. (For interpretation of the references to color in this figure legend, the reader is referred to the web version of this article.)

Table 1
Summary statistics of the field data from both the NFI and MFI plots within the study area.

	NFI	MFI
Number of sample plots	92	3937
Mean growing stock ($m^3 ha^{-1}$)	374.8	374.3
Maximum growing stock ($m^3 ha^{-1}$)	876.1	1293.0
Standard deviation of growing stock ($m^3 ha^{-1}$)	175.0	165.3

2.3. Remote sensing data

Two WV2 stereo-image pairs, i.e. four images, were used to fully cover the study area. These images were recorded under cloud-free conditions on 5 August 2013 (middle of the growing season) at approximately 10:40 a.m. local time. Detailed information about the four images is given in Table 2.

The atmospheric correction of the spectral images was performed with DLR's generic processing chain CATENA (Krauß et al., 2013; Reinartz, 2010) using the implemented ATCOR approach (Richter, 1996; Richter et al., 2006; Richter and Schläpfer, 2012). As a result, the top-of-canopy (TOC) spectral reflectance for the eight spectral bands was available for further processing. For modeling, the multispectral data were resampled to 1 m pixel size.

3. Methods

Fig. 2 illustrates the developed processing chain. The main steps are:

- computation of an image-based canopy height model (CHM),
- calculation of height and spectral explanatory variables (P) within circles of various radii (e.g. from 5 to 20 m),

Table 2

Recording parameters of the two WorldView-2 stereo-image pairs.

	Scene name	Scene acquisition date	Solar azimuth angle (degree)	Mean off-nadir view angle (degree)	Mean in track view angle (degree)	Mean cross track view angle (degree)	Scan direction
Pair 1	13AUG05103950-P2AS-13EUSI-0590-01	05.08.13	161.2	15.7	12.20	9.90	Forward
Pair 1	13AUG05104027-P2AS-13EUSI-0590-01	05.08.13	161.5	10.7	-5.50	9.19	Forward
Pair 2	13AUG05104038-P2AS-13EUSI-0590-01	05.08.13	161.2	14.0	-9.50	10.00	Reverse
Pair 2	13AUG05104003-P2AS-13EUSI-0590-01	05.08.13	161.0	12.4	6.20	10.70	Forward

- training of the Random Forests regression models for estimating growing stock at the NFI plots (including a feature selection),
- predictive model application for wall-to-wall mapping,
- validation of the model predictions at the plot and stand level using MFI data for validation.

We developed our modeling procedure in the open-source statistical software R (version 3.1.3) (R Core Team, 2015). To implement the different modeling steps, we made use of R packages *randomForest* (Liaw and Wiener, 2002), *raster* (Hijmans, 2014), *caret* (Kuhn et al., 2014) and *matrixStats* (Bengtsson, 2014).

To evaluate the impact of combining spectral with height information, three different sub-models were developed and tested:

- (1) models using solely spectral information,
- (2) models using solely height information,
- (3) models combining height and spectral information.

Additionally, as shown in Fig. 2, three different implementations ($\text{HEX}_{\text{single}}$, $\text{MW}_{\text{single}}$ and MW_{multi}) were tested for applying the developed regression models to large areas.

3.1. Computation of an image-based canopy height model

Applying image matching techniques to the stereo satellite images allows for the computation of surface heights. In the present study, we used the software package LPS eATE, integrated in ERDAS IMAGINE 2014 for this purpose. Within eATE, the area-based normalized cross-correlation method is used to identify corresponding image points. As input data, the panchromatic WV2 images with spatial resolution of 0.50 m were selected. The provided rpc (Rational polynomial coefficients) files were used for orienting the images. The image-matching processing resulted in a DSM with 1 m spatial resolution.

Canopy heights were calculated at 1 m spatial resolution as the difference between the image-based DSM and the ALS-based DTM. For the study area, an ALS-based DTM with a spatial resolution of 1 m (ALS last return density of 1.37 per m²) from a topographic mapping survey in 2009 was used for this purpose.

3.2. Masking of vegetation higher than 2 m

A vegetation mask (≥ 2 m) was derived from the WV2 data using the computed CHM (respectively, normalized DSM outside the forest) in combination with the Normalized Difference Vegetation Index (NDVI, Rouse et al., 1974) calculated from the spectral data ($\text{NDVI} = (\text{NIR} - \text{Red}) / (\text{NIR} + \text{Red})$). The suitability of these input layers to classify different land cover classes (e.g. forest, scrubs, meadows, roads or buildings) was shown before e.g. by Hollaus et al. (2005).

First, we extracted all height values above 2 m from the CHM to select all non-ground regions as suggested by e.g. Næsset (2002) or

Nilsson (1996). In the following step, vegetated regions were extracted based on the NDVI. We applied a technique described by Heinzel et al. (2008), which automatically determines a threshold based on the histogram of the NDVI values. Here, we iteratively smooth the histogram of the NDVI-values until only one local minimum remains. In consequence, the NDVI value of that minimum was used to classify vegetated and non-vegetated regions. The final vegetation mask was computed as the intersection of the non-ground regions (from the CHM) with the vegetation regions (from the NDVI image). For all further computations, only the pixels within the vegetation mask were considered.

3.3. Calculation of explanatory variables for the NFI plots

For each NFI plot with ACS field measurements, multiple circles with radii from 5 to 20 m around the plot centers were generated. For the later model application, pixel-sharp approximations of circles were used for the extraction. We extracted the pixel values of the multispectral WV2 image and the image-based CHM within the respective circles. Sets of distribution statistics, denoted as P (e.g. mean, standard deviation, and percentiles: minimum, 1st, 5th, 10th, 20th, 25th, 50th, 75th, 80th, 90th, 95th, 99th, maximum) were calculated from the extracted pixel values for each circle (120 spectral metrics and 15 height metrics each). These metrics (135 for 16 circle sizes = 2160 in total) were used as predictor variables in the subsequent Random Forests modeling.

3.4. Random Forests modeling at the NFI plot level

To model growing stock, Random Forests (RF) regression was used (Breiman, 2001). RF is a popular ensemble regression tree algorithm for multiple regression problems based on uncorrelated decision trees. For each decision tree, a new bootstrap sample is generated from the original data and at each decision node; the algorithm randomly selects a subset of the predictors as candidates for splitting. To obtain the final regression model, the results of the individual trees are averaged. The main advantages of RF are (Breiman, 2002, 2001; Hastie et al., 2009):

- variable distributions need not to be unimodal or even normally distributed,
- high-dimensional and highly correlated data sets can be processed efficiently,
- over fitting of the models is prevented,
- performance measures can be computed using only the out-of-bag (OOB) data,
- information on the importance of each input variable for the model is provided.

The fact that the model performance can be computed along the way using the OOB samples is a very appealing feature of RF. This is

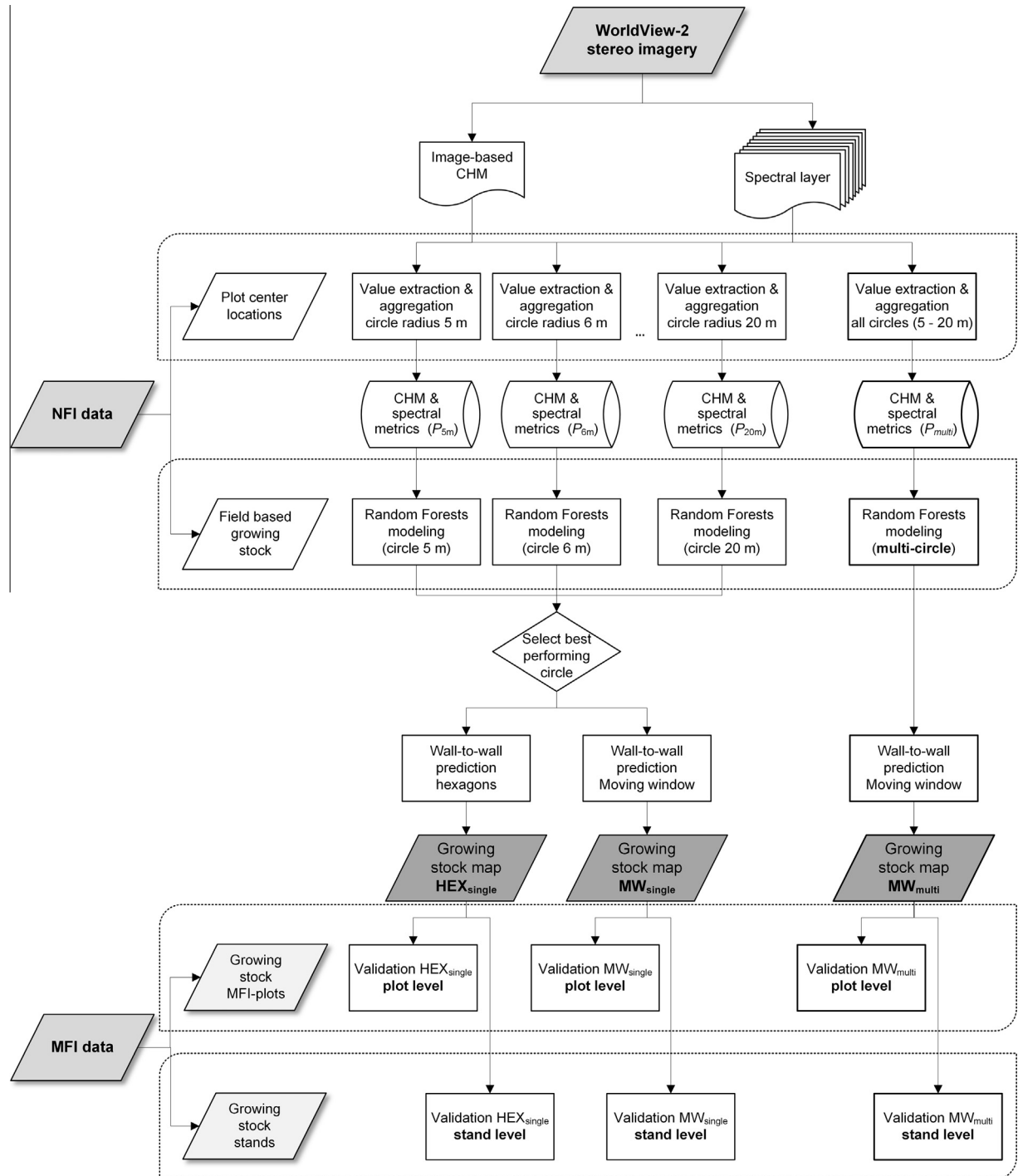


Fig. 2. Methodological workflow for the different wall-to-wall mapping approaches based on WorldView-2 stereo images and ACS National Forest Inventory (NFI) plots including validation with Management Forest Inventory (MFI) data.

possible as not all observations are included in the respective bootstraps of the individual trees. According to [Hastie et al. \(2009\)](#), the OOB error estimates are very similar to those obtained by N -fold cross-validation.

The main disadvantage of RF models is that the averaging of the single trees tends to an overestimation of small values and an underestimation of high values ([Baccini et al., 2004](#); [Horning, 2010](#); [Vanselow and Samimi, 2014](#)). Due to the underlying decision trees, it is not possible for RF to predict beyond the range of the input data.

We followed the recommendation of [Kuhn and Johnson \(2013\)](#) with regard to the estimation procedure and fixed the number of regression trees for the forest (n_{tree}) at 1000, giving a balance between computational expense and model performance. For the number of variables randomly selected from the total set of predictor variables P at each node (m_{try}), we used the default setting for regression mode ($m_{try} = P/3$), as recommended by [Breiman \(2001\)](#).

For the estimation of growing stock, different sets of explanatory variables were tested (cf. Fig. 2). We developed models using either the spectral or the height variables. Additionally, models

based on the combination of both variable sets were generated. The different approaches were applied for all 16 concentric circles separately, as well as for a dataset comprising the statistical metrics from all circles at once. Thus, in total $(16 + 1) \times 3 = 51$ different RF models were generated and evaluated.

3.4.1. Statistical assessment of models

To determine the precision and accuracy of the different models, the absolute and relative root mean squared error (RMSE), the bias (absolute and relative) and the coefficient of determination (R^2) were calculated as:

$$\text{RMSE} = \sqrt{\frac{\sum_{i=1}^n (y_i - \hat{y}_i)^2}{n}} \quad (1)$$

$$\text{RMSE}_{\text{rel}} = \frac{\text{RMSE}}{\bar{y}} \times 100 \quad (2)$$

$$\text{bias} = \frac{\sum_{i=1}^n (y_i - \hat{y}_i)}{n} \quad (3)$$

$$\text{bias}_{\text{rel}} = \frac{\text{bias}}{\bar{y}} \times 100 \quad (4)$$

$$R^2 = \frac{\sum_{i=1}^n (\hat{y}_i - \bar{y})^2}{\sum_{i=1}^n (y_i - \bar{y})^2} \quad (5)$$

where y_i is the observed value, \hat{y}_i the predicted value, \bar{y} the mean of the observed values, and n is the number of observations.

3.4.2. Feature selection

The different models incorporate large sets of WV2 explanatory variables, which are highly prone to multi-collinearity. Although RF is capable to handle high dimensional and even heavily correlated data sets, an elimination of non-relevant or redundant features can further improve the model performance (Hastie et al., 2009). We subsequently applied a backward feature selection algorithm based on the RF importance value 'Increase of Mean squared Error' (%IncMSE). This approach is similar to the recursive feature elimination procedure described in Guyon et al. (2002).

3.5. Wall-to-wall mapping

Ideally, the cell size used for a predictive application of the regression models (i.e. wall-to-wall mapping) should coincide with the plot size used for model development (White et al., 2013a; Woods et al., 2011). Following this, and considering our multi-circle approach for metrics extraction and modeling at the ACS plots, we implemented a pixel-by-pixel moving window (MW) procedure. The MW procedure generates the input layer for the RF model application to produce wall-to-wall maps. For each (central) pixel within the vegetation mask, all pixel values inside the specific circle around this pixel were extracted for all circle sizes and layers (multispectral WV2 image and the image-based CHM) and the specific metrics were calculated. We used the same pixel-sharp approximations of circles and calculated the same metrics as for the training data. In the end the required metrics (which were identified during the specific RF modeling procedures) were saved for each pixel into a multilayer raster file and the RF models were applied to these data. The MW approach was implemented both for the best performing single-circle model (MW_{single}) and for the best performing multi-circle model (MW_{multi}).

For comparison, we additionally generated a wall-to-wall growing stock map based on hexagons. Therefore, the entire study area was delineated in non-overlapping, uniform hexagons in order to

assign each pixel to exactly one hexagonal segment (Stepper et al., 2015a). The size of these hexagons (HEX_{single}) was adjusted to be the same as the area of the circle identified by the best performing single-circle model. Given the pixel-size and the desired area of the hexagonal template, there was a small trade-off between area accuracy and symmetry of the hexagon template.

The workflows for the three approaches are illustrated in Fig. 2.

3.6. Model validation

3.6.1. Validation at the plot-level

As mentioned, 3937 circular 500 m^2 inventory plots from the MFI were used as validation data set. For each plot, all modeled values inside the 500 m^2 circle were extracted from the three different wall-to-wall growing stock maps (HEX_{single} , MW_{single} , MW_{multi}). The extracted values were then averaged for each plot and compared to the field-based estimates.

3.6.2. Validation at the stand-level

Besides a validation at the plot level, the produced maps were also validated at the stand level following e.g. Rahlf et al. (2014) or Stepper et al. (2015a). For this purpose, the inventory-based growing stocks of 252 selected stands (see Section 2.2.3) were compared to the estimates from the wall-to-wall predictions (HEX_{single} , MW_{single} , MW_{multi}). To obtain the predicted stand level estimates, we selected the modeled values of all 1 m^2 pixels completely contained by the stand polygons and calculated the respective means.

4. Results

4.1. Model performance of the different approaches

Table 3 shows the OOB estimates for the three model approaches (1) spectral variables only, (2) height variables only, and (3) using a combination of spectral and height variables. The OOB estimates were computed for all 16 single-circle models separately and for the multi-circle model (last row). Only the results for the final models are presented in Table 3, i.e. the OOB estimates achieved for the models with optimized features. Feature selection generally had a positive effect compared to using all variables (not shown): the mean improvement of the RMSE was 8.0% for all single-circle models and 18.6% for the three multi-circle models.

The models solely based on spectral variables achieved R^2 values below 0.3 and relative RMSEs above 40%. Here, the multi-circle model performed best with $R^2 = 0.40$ and $\text{RMSE}_{\text{rel}} = 37.1\%$ (Fig. 3d). The spectral models were outperformed by models using only the height variables (best single-circle ($r = 12 \text{ m}$): $R^2 = 0.48$, $\text{RMSE}_{\text{rel}} = 33.5\%$; multi-circle model: $R^2 = 0.53$, $\text{RMSE}_{\text{rel}} = 31.7\%$).

The models built on the combination of both variable sets, i.e. spectral and height variables, were superior to the aforementioned separate models in terms of the model's predictive capabilities (best single-circle ($r = 15 \text{ m}$): $R^2 = 0.53$, $\text{RMSE}_{\text{rel}} = 32.0\%$, Fig. 1c). The positive effect was observed for all individual circle sizes and was particularly strong in the multi-circle model. If the explanatory variables were extracted from multiple circles, the accuracy increased considerably compared to all other models (multi-circle model: $R^2 = 0.60$, $\text{RMSE}_{\text{rel}} = 29.5\%$, Fig. 3f). Thus, the model based on a dataset comprising the height and spectral metrics from all circles at once outperformed all other tested models. This model was built with 17 remaining variables (after feature selection): 15 metrics derived from the CHM and two from the spectral data. Here, the 99th quantile computed from the digital numbers of the blue band, extracted within

Table 3

OOB performance measures for the different model approaches developed for estimating growing stock at ACS inventory plots ($n = 92$). Results are given for the different sets of explanatory variables (spectral, height, and combination), separately for each tested circle size as well as for the multi-circle approach (best approaches and multi-circle approach in bold letters).

Radius (m)	Spectral variables					Height variables					Combination (spectral + height)				
	Vars. total	Vars. selected	R^2	RMSE ($m^3 ha^{-1}$)	RMSE (%)	Vars. total	Vars. selected	R^2	RMSE ($m^3 ha^{-1}$)	RMSE (%)	Vars. Total	Vars. selected	R^2	RMSE ($m^3 ha^{-1}$)	RMSE (%)
5	120	30	0.25	152	40.7	15	5	0.39	137	36.4	135	35	0.45	130	34.6
6	120	10	0.27	150	40.1	15	5	0.41	135	35.9	135	35	0.42	133	35.4
7	120	13	0.16	160	42.7	15	7	0.41	135	36.1	135	17	0.43	132	35.1
8	120	13	0.12	164	43.6	15	9	0.42	134	35.8	135	3	0.46	129	34.3
9	120	5	0.08	168	44.9	15	7	0.42	133	35.5	135	14	0.45	129	34.5
10	120	2	0.13	164	43.6	15	5	0.46	128	34.1	135	4	0.48	126	33.7
11	120	5	0.09	167	44.6	15	1	0.47	130	34.7	135	9	0.48	126	33.6
12	120	5	0.04	172	45.8	15	2	0.48	125	33.5	135	22	0.49	124	33.0
13	120	3	0.12	165	44.1	15	5	0.47	126	33.7	135	12	0.51	121	32.4
14	120	4	0.07	168	44.9	15	13	0.42	133	35.5	135	11	0.50	124	33.0
15	120	3	0.17	160	42.6	15	5	0.43	131	35.1	135	12	0.53	120	32.0
16	120	3	0.12	164	43.8	15	4	0.44	130	34.6	135	11	0.49	125	33.3
17	120	9	0.10	166	44.3	15	4	0.44	130	34.8	135	10	0.46	128	34.2
18	120	3	0.12	165	43.9	15	2	0.43	131	35.0	135	10	0.44	130	34.7
19	120	2	0.09	169	45.2	15	5	0.39	136	36.4	135	10	0.44	130	34.8
20	120	2	0.10	167	44.7	15	2	0.46	128	34.1	135	1	0.42	134	35.7
Multi	1920	16	0.40	139	37.1	240	20	0.53	119	31.7	2160	17	0.60	110	29.5

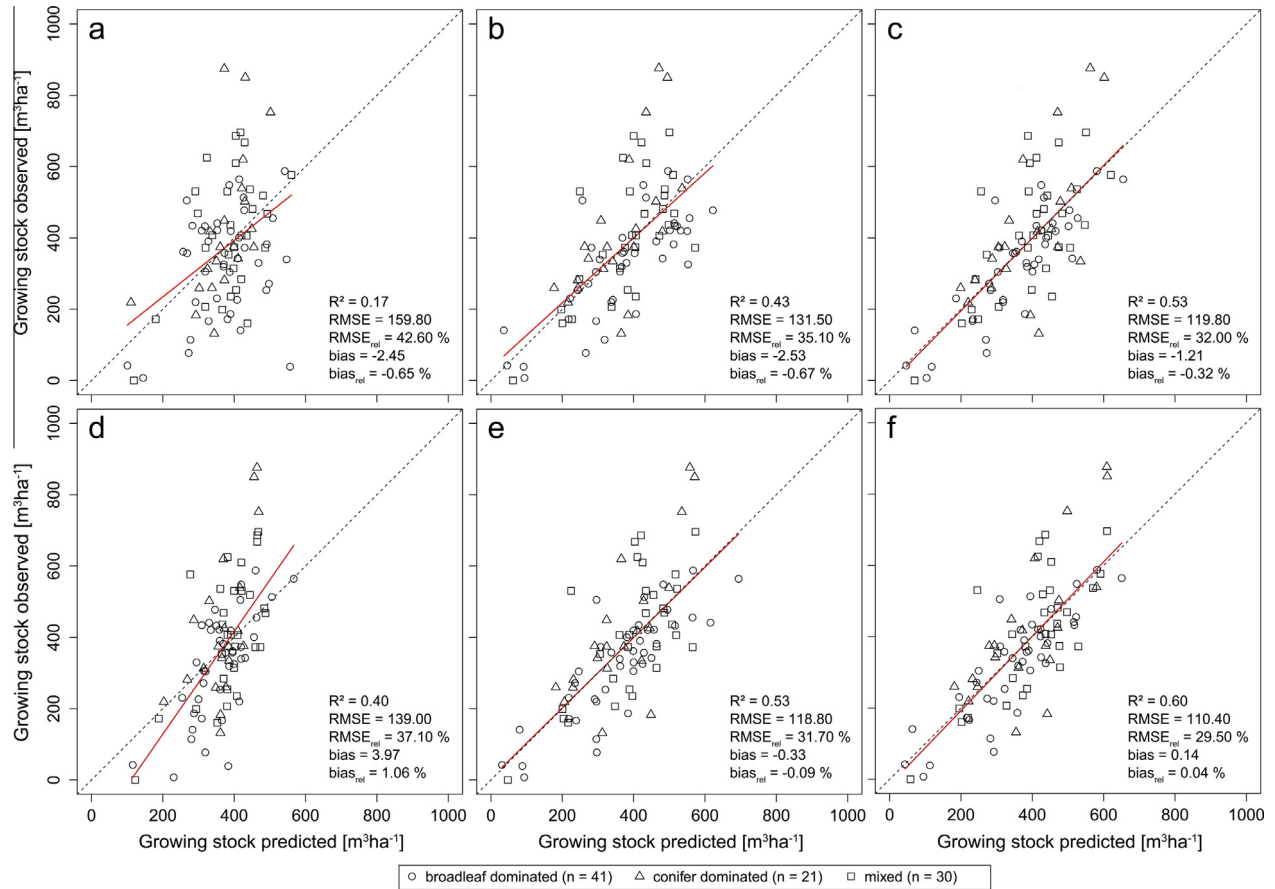


Fig. 3. Scatterplots of predicted vs. observed growing stock using the explanatory variables based on spectral information (a and d), height information (b and e), and the combination of both (c and f). The subfigures in the first row (a–c) show the results for the single-circle models with radius 15 m, the bottom-row subfigures (d–f) the results for the multi-circle models.

the 13 m radius circles, obtained the highest importance scores. The CHM-derived height metrics 25th quantile (12 m radius circle) and 75th quantile (7 m radius circle) gained almost the same score levels. Next to these variables also different 50th quantiles from the CHM (of various circle radii from 7 m to 20 m) and the 10th

quantile computed from the digital numbers of the green band (15 m circle radius) were selected.

The results from the OOB performance measures were confirmed in the scatterplots of predicted vs. observed growing stock (Fig. 3). In these scatterplots, the observed values are given on

the y-axis and the predicted on the x-axis following Piñeiro et al. (2008). Separate symbols were used for broadleaf dominated, conifer dominated, and mixed forest types. Forest types were classified according to the actual proportions of the total growing stock, however revealed no tendencies with regards to the estimation of growing stock.

4.2. Wall-to-wall model application

The results of the wall-to-wall model application of the different methods ($\text{HEX}_{\text{single}}$, $\text{MW}_{\text{single}}$, MW_{multi}) are shown in Fig. 4 for a subset of the study area together with a CIR composite of a WV2 image, the CHM and the vegetation mask. Regarding the three growing stock maps, a general coincidence between the $\text{HEX}_{\text{single}}$ map and the two MW maps is recognizable. However, the MW approaches (e and f) are capable to better preserve the forest structure when mapping growing stock for the area. Using the $\text{HEX}_{\text{single}}$ method (d), the predicted growing stocks tend to be more smoothed, not capturing the extremes and changes at stand boundaries well. Regarding the two MW maps, the differences appear to be small.

For the total forest enterprise area the three wall-to-wall methods reached mean growing stock values of $375 \text{ m}^3 \text{ ha}^{-1}$ ($\text{HEX}_{\text{single}}$), $394 \text{ m}^3 \text{ ha}^{-1}$ ($\text{MW}_{\text{single}}$) and $380 \text{ m}^3 \text{ ha}^{-1}$ (MW_{multi}). The aggregated growing stock estimates are shown in Fig. 5 for the delineated forest stands within the state owned land (MW_{multi} approach). This map reflects the great variability of developmental stages of the forest stands within the study area. Modeled stand-wise growing stocks range from 50 to more than $450 \text{ m}^3 \text{ ha}^{-1}$.

4.3. Model validation

The scatterplots in Fig. 6 show the predicted growing stock values of the different methods ($\text{HEX}_{\text{single}}$, $\text{MW}_{\text{single}}$, MW_{multi}) vs. the observed growing stock values from the 3937 MFI field measurements. Principally, the scatter is similar for the three methods, showing comparable deviations from the 1:1 line. Irrespective of the approach used, a systematic underestimation can be observed for inventory plots with high growing stocks of more than about $700 \text{ m}^3 \text{ ha}^{-1}$. Contrary, the observed growing stocks at plots without or with very little stocking tend to be overestimated by all approaches.

The accuracy assessment using the MFI data (Fig. 6) generally shows RMSE values only slightly higher than the OOB estimates of the established RF regression models. For all approaches, a slight negative bias is observed, i.e. the models overestimate the actual measurements to some extent. The R^2 values with a maximum of 0.44 for the MW_{multi} approach, however, are significantly lower than the corresponding OOB estimates ($R^2 = 0.60$).

Fig. 7 shows the predicted stand level estimates vs. the averaged observed growing stocks for 252 validation stands. Only stands containing at least five MFI plots were used for validation. As a result of the aggregation to the stand level, the scatter of predicted vs. observed values was substantially reduced for all approaches. In contrast to the plot-level validation, no systematic under or overestimation is visible for the stands at the upper and lower distribution edges. The calculated RMSE values at the stand level were reduced by more than half compared to the plot-level RMSEs. Again, the MW approaches outperformed the $\text{HEX}_{\text{single}}$ approach in terms of the achieved model precision with relative RMSEs of 14.8% ($\text{MW}_{\text{single}}$) and 15.1% (MW_{multi}) compared to 16.2% ($\text{HEX}_{\text{single}}$).

4.4. Iterative feature elimination procedure

The results presented thus far were obtained using a feature selection approach. In the case of the overall best performing model – the multi-circle approach using the combination of spectral and height information – the feature selection resulted in a final subset of 17 variables (from 2160 computed variables). The selected algorithm starts with the full set of variables and continuously removes the least important one in a sequential mode. At the end, the model with the best performance based on the least number of input variables is identified.

To evaluate the efficacy of the implemented iterative strategy, we compared the performance of the “optimum” model (vertical line in Fig. 8) to a large number of randomly chosen models (2.5 million), each based on 17 randomly selected variables. For the selection of the 17 variables, the 100 most important variables of the full model were considered. The mean R^2 of these models with randomly drawn predictors was 0.53 with a negative skew (Fig. 8). The best model based on a randomly selected variable set was slightly better than the model based on the backward stepwise elimination ($R^2 = 0.62$ vs. 0.60). As shown in Fig. 8, only 0.12% of the 2.5 million models performed better than the one with the variables remaining after the sequential selection. However, running such a large number of simulations, takes a considerable amount of time, whereas the proposed feature selection approach is very time-efficient.

5. Discussion

5.1. Stereo satellite images as alternative to airborne stereo image data

It is well known that tree height is positively correlated with growing stock (Pretzsch, 2010). Nevertheless, supplying the modeling procedure with spectral data in addition to height data can increase the performance. This has been shown by Kattenborn et al. (2015), Stepper et al. (2015a) and Van Ewijk et al. (2014) who demonstrated that the additional spectral information can be incorporated as indication of tree species (and age class) groups. Maack et al. (2015) obtained the best results for biomass estimation with combined spectral and CHM metrics. Our modeling results for estimating growing stock based on WorldView-2 (WV2) data confirm these findings. For example, comparing the OOB performance measures of the different multi-circle models, the model based solely on spectral variables achieved an RMSE_{rel} of 37.1%, whereas the model based on height variables achieved an RMSE_{rel} of 31.7%. However, by combining both variable sets (height plus spectral), the RMSE_{rel} was reduced to 29.5%.

Straub et al. (2013b) reported an RMSE_{rel} of 44.4% for estimating growing stock in a complex mixed forest using solely height data derived from WV2. In comparison to this study our modeling results are considerably better. These differences can be assigned to different forest structures and species compositions. Nonetheless, in the current study we could reveal some additional positive contributions to modeling by combining spectral and height information.

Very positive results were also obtained by Kattenborn et al. (2015) for a relatively homogeneous forest. Here, the combined use of WV2 height and Hyperion spectral data resulted in an RMSE_{rel} of 24.8% for biomass at the plot level. Compared to these results, our model performances are somewhat worse. Again, we attribute these differences mostly to the different forest types.

To the best of our knowledge, these are so far the only studies using WV2 stereo data for estimating forest attributes such as

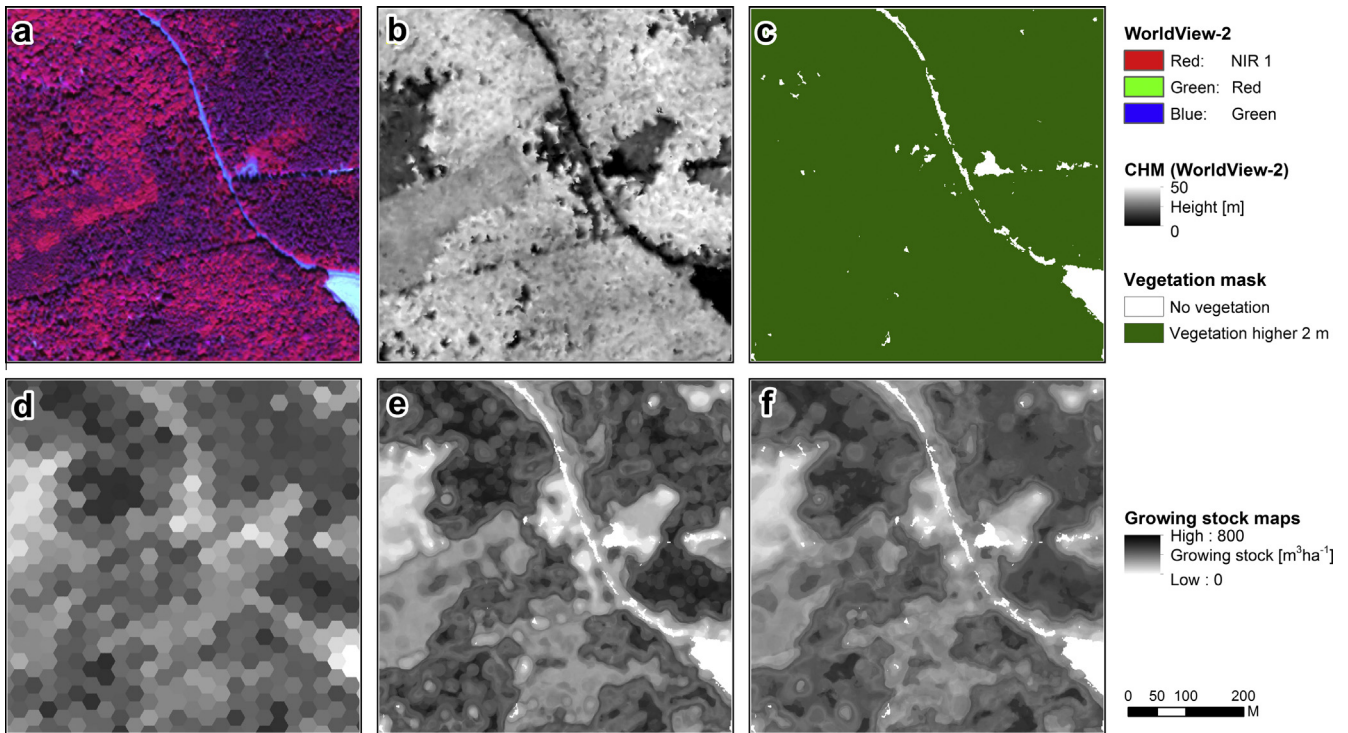


Fig. 4. Illustration of the different approaches for wall-to-wall mapping of the NFI ground measured growing stocks. (a) WorldView-2 data visualized in CIR band combination, (b) image-based CHM, (c) computed vegetation mask defining the area where MW mapping is applied, (d) hexagon-based wall-to-wall mapping (HEX_{single}), (e) MW wall-to-wall mapping using single-best-circle (MW_{single}), and (f) MW wall-to-wall mapping using multiple circles (MW_{multi}).

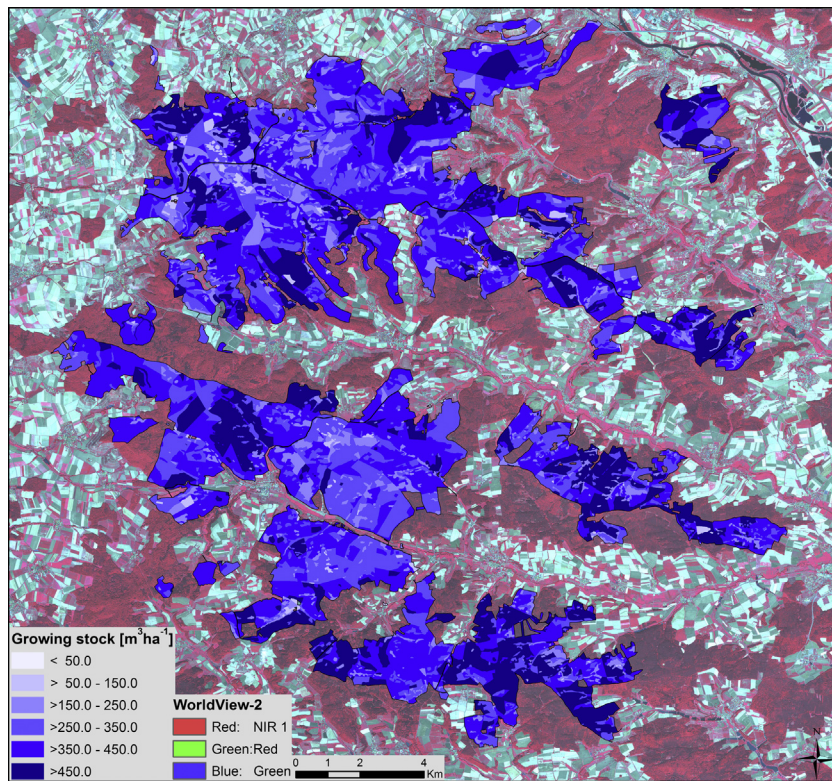


Fig. 5. Map of the growing stock estimates aggregated at the stand level for the state-owned land based on the original 1 m^2 maps obtained from the MW_{multi} approach.

growing stock. Due to the appealing nature of the results, we suggest further investigation of the potential of WV2 and other stereo

satellite data. Special attention should be paid to the combined use of height and spectral information.

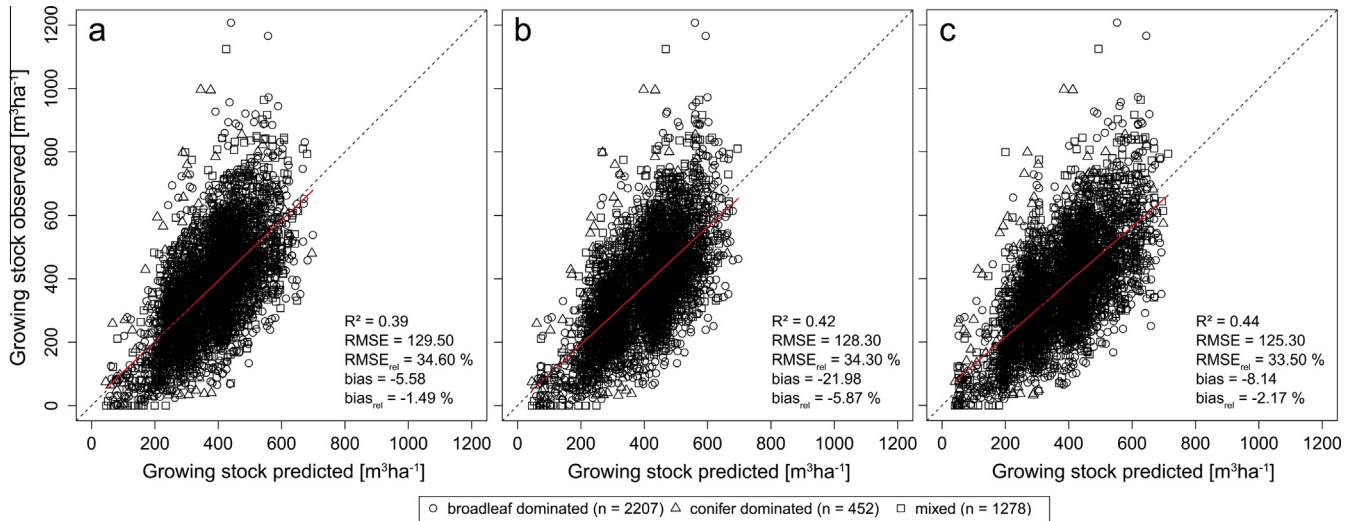


Fig. 6. Scatterplots of predicted growing stock vs. observed growing stock for the three different wall-to-wall mapping approaches, (a) HEX_{single}, (b) MW_{single}, and (c) MW_{multi}. As independent validation data set, the field measurements of the MFI were used.

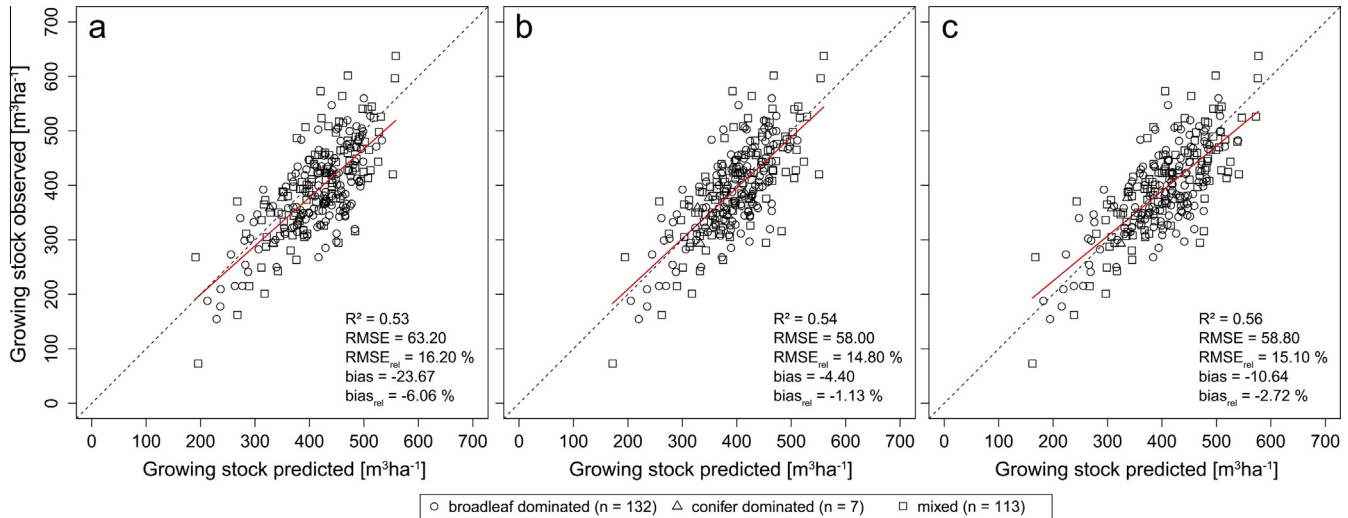


Fig. 7. Scatterplots of predicted growing stock vs. observed growing stock for the three different wall-to-wall mapping approaches, (a) HEX_{single}, (b) MW_{single}, and (c) MW_{multi} for 252 validation stands containing at least five MFI plots.

5.2. Use of angle-count sampling field measurements for model training

NFI programs are installed as long term monitoring projects and the data are acquired following standardized instructions. As the NFIs are conducted by national authorities, these data are generally publicly available and are of high quality. In Central Europe, the inventory design of the NFIs relies often on probability-based sampling (ACS) (Tomppo et al., 2010). However, most published remote sensing approaches follow the area-based approach using fixed area field sample plots for model training (Næsset, 2002; White et al., 2013a). Thus, the challenge we faced in this study was to overcome the drawback of ACS-based field measurements for linking them to the remote sensing data, as the spatial extent of each plot is different. The proposed method is potentially very valuable for large-area applications integrating remote sensing data and NFI surveys.

Hollaus et al. (2009) and Immitzer (2013) tried to cope with this problem by fitting circles with different radii to the ACS plots and selecting the best performing model (circle), i.e. the model with the

lowest RMSE. However, doing so only partly meets the design of ACS plots, as there are always trees either included or excluded from the “best fitting circle”. We demonstrate that it is advantageous to extract and combine the information from multiple circles rather than attempting to identify one “optimum” circle size. This can be seen in Table 3, which confirms that the developed multi-circle approach outperforms all models based on one specific circle. For example, when using the combination of height and spectral metrics, the RMSEs (OOB) were reduced for the multi-circle model by 2.5 percent points compared to the best single-circle model (29.5% vs. 32.0%).

5.3. Random Forests for modeling the growing stock

Different studies published recently have shown the potential of Random Forests (RF) regression for growing stock modeling (e.g. Kattenborn et al., 2015; Pitt et al., 2014; Stepper et al., 2015a). This was confirmed by our study showing that the non-parametric regression method RF was successfully applied for estimating the growing stock. The scatterplots in Fig. 3 show

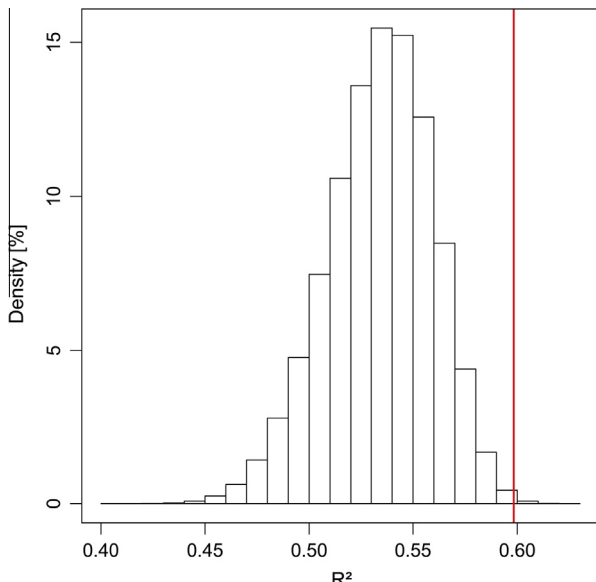


Fig. 8. Histogram of R^2 values for 2.5 million models, each based on a set of 17 randomly selected variables; the vertical line indicates the R^2 value of the model based on the variables selected with the developed feature elimination algorithm.

the predicted vs. the observed growing stock values for the NFI plots. The graphs confirm that the RF models are not biased. However, they unveil the common – and well-known – disadvantage of all decision tree based models; the overestimation of small and underestimation of high values respectively (Baccini et al., 2004; Vanselow and Samimi, 2014). This can be attributed to the bootstrapping approach, which ensures that different training samples are used for various decision trees. The disadvantage is that extreme values are often ‘out-of-bag’ and therefore cannot positively contribute to the ‘learning phase’. Nonetheless, the scatterplots for growing stock at the NFI plot level (and in particular at the stand level) show a good correlation between predicted and observed values.

5.4. Feature selection to improve model performance

Although it is commonly agreed that RF can handle many highly correlated variables as well as non-informative predictors, we applied a feature selection algorithm to reduce the number of input variables. Kuhn and Johnson (2013) stated for RF, that the inclusion of non-informative predictors has no serious influence on the overall regression model. But due to the random selection of predictors for splitting at each node (m_{try}), a large portion of non-informative predictors can coerce the final model to include unimportant predictors and thus, the model performance can be constrained. Additionally, from a practical point of view, calculating a large number of variables is computationally burdensome, especially when following the proposed multi-circle approach (spectral and height metrics from multiple circles). Having both aspects in mind, by installing a well-functioning feature reduction procedure, we can achieve better and more stable modeling results based on relative small subsets of variables.

Our approach can be assigned to the wrapper methods, as multiple models are evaluated to find the optimal variable set for maximizing model performance (a detailed description of the different feature selection categories can be found in Kuhn and Johnson (2013)). In our case, the search algorithm utilizes the RF model as base learner and the RMSE as objective function to be optimized. One drawback of the proposed method is that it can be trapped in local minima and consequently the best variable subset is not

found. To overcome this disadvantage, all possible subset combinations have to be tested, which is hardly feasible. As shown in Fig. 8, our approach was able to select a very well performing feature subset, outperforming the overwhelming majority of randomly selected subsets (e.g. 2.5 Mio different models). This is especially important for practical applications, as time can be saved during model training and application.

5.5. Wall-to-wall mapping and model validation

Both methods, i.e. the fixed prediction units in hexagonal shape as well as the moving window approach predicting on a 1 m² basis, were successfully applied to generate wall-to-wall estimates of growing stock. For forest planning purpose such as assessment of annual yield, the mean growing stock is of interest. The three models achieved a mean growing stock for the entire forest enterprise of about 380 m³ ha⁻¹ which is very close to the value calculated from the MFI data (374 m³ ha⁻¹), not used for model training. The moving window approaches, both the MW_{single} and the MW_{multi}, resulted in spatially detailed maps of growing stock. As displayed in Fig. 4, the moving window approaches are capable to better preserve the forest structure compared to the HEX_{single} approach. With regard to practical applications and as a supporting tool for forest planning and management, the computed maps are of great value. The aggregated stand level estimates of growing stock offer further advantages for integrating the presented approaches into existing forest planning and monitoring practices. The spatially explicit estimates of growing stock for the different stands, in combination with the CHM giving insights into the status of canopy height and closure, can help forest practitioners to identify stands, which have to be prioritized for silvicultural treatments in order to comply with certain tending objectives.

In the current study, we had the opportunity to evaluate our predictive models using inventory data from the MFI as validation data set. Thus, we were able to assess the reliability of the OOB estimates gained from the RF-modeling. Fortunately, the 92 plot measurements of the sparse NFI grid provided a reasonable characterization of the growing stock within the study area, resulting in nearly exact same mean values as derived from the 3937 MFI plot measurements as well as comparable standard deviations (cf. Table 1). Thus, the necessary prerequisite for a meaningful prediction is fulfilled. Due to lower maximum value of the NFI measurements compared to the MFI, the predictive models based on the NFI data are partially restricted looking at the top end of the observed growing stocks. This is especially true as RF is not able to extrapolate beyond the range of values used for training.

The relative RMSE values computed for the prediction of growing stock at the 3937 MFI plots (HEX_{single}: 34.6%, MW_{single}: 34.3%, MW_{multi}: 33.5%) are only slightly higher than the OOB estimates (best single circle: 32.0%, multi-circle: 29.5%). These results confirm the assumption, that using the OOB estimates gives a reasonable measure of the model performance. The results further approved the predictive capacity of the RF models, not being overly fitted to the training data.

Recently, Stepper et al. (2015a) published results from a study conducted in the northern subarea of the current study area. For RF models based on height and spectral information from aerial images, they achieved a minimum relative RMSE of 30.9% at the plot level (cross-validated). Using this as a reference, and looking at the very similar results in the current study, we could demonstrate that the combination of NFI field plot data and stereo WV2 remote sensing data is feasible for modeling growing stock at the plot level in this forest environment. However, in similarity to the study of Stepper et al. (2015a), when looking at the scatterplots in Fig. 6, a systematic underestimation for MFI plots with growing stock values higher than approx. 700 m³ ha⁻¹ can be observed. We

attribute this to (a) the poor availability of NFI plots with high growing stocks and (b) to the known shortcoming of the non-parametric RF approach when estimating values next to the Minimum or Maximum of the data range.

Additionally to the validation at the MFI plot level, we scrutinized the wall-to-wall maps of growing stock produced at the forest stand level. As a result of aggregation to the stand level, the RMSEs were reduced significantly compared to the plot-level estimates. This is similar to the findings reported e.g. by Gobakken et al. (2015), Rahlf et al. (2014) and Stepper et al. (2015a). Moreover, the achieved relative RMSEs of 14.8–16.2% for the different mapping approaches are comparable to those reported in Stepper et al. (2015a) – they achieved a relative RMSE at the stand level of 13.9% for a subset of the currently used stands. The issue of underestimating high growing stocks, as discussed above for the plot level, was not found at the stand level (scatterplots in Fig. 7). We explain this, at least in part, with the integration effect at the stand level, i.e. averaging the high resolution predictions to a coarser scale.

The achieved results, especially when looking at the model validation using the MFI data as well as the forest stands, highlight the great potential of WV2 derived height and spectral data for estimating growing stock. In addition, they further underline that image-based height data (airborne and spaceborne) should be taken into consideration as an alternative to ALS for these kinds of application.

6. Conclusions

In this study, we demonstrated the potential of WorldView-2 (WV2) stereo data together with National Forest Inventory (NFI) field plots to generate maps of the growing stock. These maps were produced at 1 m spatial resolution using RF-regression.

Several main conclusions can be drawn from our study:

- Stereo images from high resolution satellites such as WV2 can be used to compute detailed canopy height information. The satellite-derived canopy heights in combination with the available spectral data were successfully used in the estimation of growing stock.
- The combined use of spectral and height information outperformed the sole use of either spectral or height data.
- The developed method with multiple circles was able to generate spatially detailed and accurate maps displaying the distribution of growing stock within the forest.
- The developed moving window (MW) approach for map generation proved very efficient and outperformed an approach based on fixed hexagons.
- An aggregation of the estimated growing stocks to larger units (e.g. from plot to stand level) further reduced the estimation error.

Our results underline the great potential of the developed moving window method as an area-based mapping approach, especially when angle-count field inventory plots are used for model training. By overcoming the fixed-area reference prerequisite, it is possible to use ACS based field measurements, such as the German NFI plots, without approximating one specific circle. This is especially important with regards to the standardized measurements and the availability of these data throughout the country.

Acknowledgements

The authors thank the Bavarian state forest enterprise (BaySF) for providing the MFI data and operational unit information,

H.J. Klemmt for providing the NFI data and the Bavarian Surveying Administration for providing the ALS-based DTM data used in this study. Our thanks are due to the German Remote Sensing Data Center (DFD) of the German Aerospace Center (DLR) for efficient collaboration; in particular, our thanks go to Anne Reichmuth for the preprocessing of the WV2 data. We would like to acknowledge Valerie Koch (BOKU, Vienna) for the DSM generation. This research was partially funded by a grant (project E53: Sapex_SAT: Proof of concept of a large-scale characterization of forest stands menaced by climate change and regionalization of large scale inventories on large areas) from the Bavarian State Ministry of Food, Agriculture and Forestry (in German: Bayerisches Staatsministerium für Ernährung, Landwirtschaft und Forsten), which is gratefully acknowledged. The authors are grateful to two anonymous reviewers who offered valuable recommendations and comments and to Ms. Brynn McMillan for English editing.

References

- Baccini, A., Friedl, M.A., Woodcock, C.E., Warbington, R., 2004. Forest biomass estimation over regional scales using multisource data. *Geophys. Res. Lett.* 31, L10501. <http://dx.doi.org/10.1029/2004GL019782>.
- BaySF, 2011. Richtlinie für die mittel- und langfristige Forstbetriebsplanung in den Bayerischen Staatsforsten (Forsteinrichtungsrichtlinie FER). Bayerische Staatsforsten, Regensburg.
- Bengtsson, R.J., 2014. matrixStats: Methods that Apply to Rows and Columns of a Matrix. R Package Version 0.10.0. R Package.
- Bitterlich, W., 1948. Die Winkelzählprobe. *Allg. Forst Holzwirtsch. Ztg.* 59, 1–2.
- BMEL, 2015. Surveying the Forest – Bundeswaldinventur. BMEL, Bonn.
- BMELV (Ed.), 2011. Survey Instructions for the 3rd National Forest Inventory (2011–2012), second ed. BMELV, Bonn.
- Breidenbach, J., Astrup, R., 2012. Small area estimation of forest attributes in the Norwegian National Forest Inventory. *Eur. J. For. Res.* 131, 1255–1267. <http://dx.doi.org/10.1007/s10342-012-0596-7>.
- Breiman, L., 2002. Manual on Setting Up, Using, and Understanding Random Forests. V3.1.
- Breiman, L., 2001. Random forests. *Mach. Learn.* 45, 5–32. <http://dx.doi.org/10.1023/A:1010933404324>.
- Chirici, G., Barbati, A., Corona, P., Marchetti, M., Travaglini, D., Maselli, F., Bertini, R., 2008. Non-parametric and parametric methods using satellite images for estimating growing stock volume in alpine and Mediterranean forest ecosystems. *Remote Sens. Environ.* 112, 2686–2700. <http://dx.doi.org/10.1016/j.rse.2008.01.002>.
- Chirici, G., Corona, P., Marchetti, M., Mastronardi, A., Maselli, F., Bottai, L., Travaglini, D., 2012. K-NN FOREST: a software for the non-parametric prediction and mapping of environmental variables by the k-Nearest Neighbors algorithm. *Eur. J. Remote Sens.* 45, 433–442. <http://dx.doi.org/10.5721/EuJRS20124536>.
- Falkowski, M.J., Wulder, M.A., White, J.C., Gillis, M.D., 2009. Supporting large-area, sample-based forest inventories with very high spatial resolution satellite imagery. *Prog. Phys. Geogr.* 33, 403–423. <http://dx.doi.org/10.1177/0309133309342643>.
- Gallaun, H., Zanchi, G., Nabuurs, G.-J., Hengeveld, G., Schardt, M., Verkerk, P.J., 2010. EU-wide maps of growing stock and above-ground biomass in forests based on remote sensing and field measurements. *For. Ecol. Manage.* 260, 252–261. <http://dx.doi.org/10.1016/j.foreco.2009.10.011>.
- Gobakken, T., Bollandsås, O.M., Næsset, E., 2015. Comparing biophysical forest characteristics estimated from photogrammetric matching of aerial images and airborne laser scanning data. *Scand. J. For. Res.* 30, 73–86. <http://dx.doi.org/10.1080/02827581.2014.961954>.
- Guyon, I., Weston, J., Barnhill, S., Vapnik, V., 2002. Gene selection for cancer classification using support vector machines. *Mach. Learn.* 46, 389–422. <http://dx.doi.org/10.1023/A:1012487302797>.
- Hastie, T., Tibshirani, R., Friedman, J., 2009. *The Elements of Statistical Learning: Data Mining, Inference, and Prediction*, second ed. Springer, New York.
- Heinzel, J.N., Weinacker, H., Koch, B., 2008. Full automatic detection of tree species based on delineated single tree crowns – a data fusion approach for airborne laser scanning data and aerial photographs. In: SilviLaser 8th International Conference on LiDAR Applications in Forest Assessment and Inventory. Presented at the SilviLaser 8th International Conference on LiDAR Applications in Forest Assessment and Inventory, Edinburgh, UK, pp. 76–85.
- Hijmans, R.J., 2014. Raster: Geographic Data Analysis and Modeling. R Package.
- Hobi, M.L., Ginzler, C., 2012. Accuracy assessment of digital surface models based on WorldView-2 and ADS80 stereo remote sensing data. *Sensors* 12, 6347–6368. <http://dx.doi.org/10.3390/s120506347>.
- Hollaus, M., Wagner, W., Kraus, K., 2005. Airborne laser scanning and usefulness for hydrological models. *Adv. Geosci.* 5, 57–63.
- Hollaus, M., Wagner, W., Schadauer, K., Maier, B., Gabler, K., 2009. Growing stock estimation for alpine forests in Austria: a robust lidar-based approach. *Can. J. For. Res.* 39, 1387–1400.

- Horning, N., 2010. Random forests: an algorithm for image classification and generation of continuous fields data sets. In: Presented at the International Conference on GeoInformatics for Spatial Infrastructure Development in Earth and Allied Sciences, Hanoi, Vietnam.
- Immitzer, M., 2013. Auswertung von Airborne-Laser-Scanning-Daten für die Ableitung des Holzvorrates im Lehrforst der Universität für Bodenkultur. Master Thesis. University of Natural Resources and Life Sciences, Vienna.
- Immitzer, M., Atzberger, C., 2014. Early detection of bark beetle infestation in Norway spruce (*Picea abies* L.) using WorldView-2 data. *Photogramm. Fernerkund. Geoinform.* 2014, 351–367.
- Immitzer, M., Atzberger, C., Koukal, T., 2012a. Tree species classification with random forest using very high spatial resolution 8-band WorldView-2 satellite data. *Remote Sens.* 4, 2661–2693. <http://dx.doi.org/10.3390/rs4092661>.
- Immitzer, M., Atzberger, C., Koukal, T., 2012b. Eignung von WorldView-2 Satellitenbildern für die Baumartenklassifizierung unter besonderer Berücksichtigung der vier neuen Spektralkanäle. *Photogramm. Fernerkund. Geoinform.* 5, 573–588. <http://dx.doi.org/10.1127/1432-8364/2012/0140>.
- Kändler, G., 2006. The design of the second German National Forest Inventory. In: Proceedings of the Eighth Annual Forest Inventory and Analysis Symposium. Presented at the Forest Inventory and Analysis Symposium, 16–19 October, Monterey, CA, pp. 19–24.
- Kattenborn, T., Maack, J., Fassnacht, F., Enßle, F., Ermert, J., Koch, B., 2015. Mapping forest biomass from space – fusion of hyperspectral EO1-hyperion data and Tandem-X and WorldView-2 canopy height models. *Int. J. Appl. Earth Obs. Geoinform.* 35 (B), 359–367. <http://dx.doi.org/10.1016/j.jag.2014.10.008>.
- Koukal, T., Atzberger, C., Schneider, W., 2014. Evaluation of semi-empirical BRDF models inverted against multi-angle data from a digital airborne frame camera for enhancing forest type classification. *Remote Sens. Environ.* 151, 27–43. <http://dx.doi.org/10.1016/j.rse.2013.12.014> (Special Issue on 2012 ForestSAT).
- Koukal, T., Suppan, F., Schneider, W., 2007. The impact of relative radiometric calibration on the accuracy of kNN-predictions of forest attributes. *Remote Sens. Environ.* 110, 431–437. <http://dx.doi.org/10.1016/j.rse.2006.08.016> (ForestSAT Special Issue ForestSAT 2005 Conference “Operational tools in forestry using remote sensing techniques”).
- Krauß, T., d’Angelo, P., Schneider, M., Gstaiger, V., 2013. The fully automatic optical processing system CATENA at DLR. *ISPRS – Int. Arch. Photogramm. Remote Sens. Spat. Inform. Sci.* XL-1/W1, 177–183. <http://dx.doi.org/10.5194/isprarchives-XL-1-W1-177-2013>.
- Kuhn, M., Johnson, K., 2013. *Applied Predictive Modeling*. Springer.
- Kuhn, M., Wing, J., Weston, S., Williams, A., Keefer, C., Engelhardt, A., Cooper, T., Mayer, Z., 2014. caret: Classification and Regression Training. R Package.
- van Laar, A., Akça, A., 2007. *Forest mensuration,.. Managing Forest Ecosystems*, second ed. Springer, Dordrecht (completely rev. and supplemented. ed.).
- Liaw, A., Wiener, M., 2002. Classification and regression by randomForest. *R News* 2, 18–22.
- Maack, J., Kattenborn, T., Fassnacht, F., Enßle, F., Hernández, J., Corvalán, P., Koch, B., 2015. Modeling forest biomass using Very-High-Resolution data – combining textural, spectral and photogrammetric predictors derived from spaceborne stereo images. *Eur. J. Remote Sens.*, 245–261 <http://dx.doi.org/10.5721/EuJRS20154814>.
- Maltamo, M., Malinen, J., Packalén, P., Suvanto, A., Kangas, J., 2006. Nonparametric estimation of stem volume using airborne laser scanning, aerial photography, and stand-register data. *Can. J. For. Res.* 36, 426–436. <http://dx.doi.org/10.1139/x05-246>.
- Maltamo, M., Næsset, E., Vauhkonen, J. (Eds.), 2014. *Forestry Applications of Airborne Laser Scanning, Managing Forest Ecosystems*. Springer, Netherlands, Dordrecht.
- Maltamo, M., Packalén, P., Kallio, E., Kangas, J., Uuttera, J., Heikkilä, J., 2011. Airborne laser scanning based stand level management inventory in Finland. In: Proceedings of SilviLaser 2011. Presented at the 11th International Conference on LiDAR Applications for Assessing Forest Ecosystems, 16–20 October, Conference Secretariat, Hobart, Australia, pp. 1–9.
- Maltamo, M., Packalén, P., Suvanto, A., Korhonen, K.T., Mehtätalo, L., Hyvönen, P., 2009. Combining ALS and NFI training data for forest management planning: a case study in Kuortane, Western Finland. *Eur. J. For. Res.* 128, 305–317. <http://dx.doi.org/10.1007/s10342-009-0266-6>.
- Masek, J.G., Hayes, D.J., Joseph Hughes, M., Healey, S.P., Turner, D.P., 2015. The role of remote sensing in process-scaling studies of managed forest ecosystems. *For. Ecol. Manage.* <http://dx.doi.org/10.1016/j.foreco.2015.05.032>.
- Maselli, F., Chiesi, M., Mura, M., Marchetti, M., Corona, P., Chirici, G., 2014. Combination of optical and LiDAR satellite imagery with forest inventory data to improve wall-to-wall assessment of growing stock in Italy. *Int. J. Appl. Earth Obs. Geoinform.* 26, 377–386. <http://dx.doi.org/10.1016/j.jag.2013.09.001>.
- McRoberts, R.E., Andersen, H.-E., Næsset, E., 2014a. Using airborne laser scanning data to support forest sample surveys. In: Maltamo, M., Næsset, E., Vauhkonen, J. (Eds.), *Forestry Applications of Airborne Laser Scanning, Managing Forest Ecosystems*. Springer, Netherlands, pp. 269–292.
- McRoberts, R.E., Bollandsås, O.M., Næsset, E., 2014b. Modeling and estimating change. In: Maltamo, M., Næsset, E., Vauhkonen, J. (Eds.), *Forestry Applications of Airborne Laser Scanning, Managing Forest Ecosystems*. Springer, Netherlands, pp. 293–313.
- McRoberts, R.E., Liknes, G.C., Domke, G.M., 2014c. Using a remote sensing-based percent tree cover map to enhance forest inventory estimation. *For. Ecol. Manage.* 331, 12–18. <http://dx.doi.org/10.1016/j.foreco.2014.07.025>.
- McRoberts, R.E., Næsset, E., Gobakken, T., 2015. Optimizing the k-Nearest neighbors technique for estimating forest aboveground biomass using airborne laser scanning data. *Remote Sens. Environ.* 163, 13–22. <http://dx.doi.org/10.1016/j.rse.2015.02.026>.
- McRoberts, R.E., Nelson, M.D., Wendt, D.G., 2002. Stratified estimation of forest area using satellite imagery, inventory data, and the k-Nearest Neighbors technique. *Remote Sens. Environ.* 82, 457–468. [http://dx.doi.org/10.1016/S0034-4257\(02\)00064-0](http://dx.doi.org/10.1016/S0034-4257(02)00064-0).
- McRoberts, R.E., Tomppo, E.O., 2007. Remote sensing support for national forest inventories. *Remote Sens. Environ.* 110, 412–419. <http://dx.doi.org/10.1016/j.rse.2006.09.034>.
- Mergner, U., 2013. *Exkursionsführer Forstbetrieb Ebrach*. BaySF, Regensburg.
- Næsset, E., 2014. *Area-based inventory in Norway – from innovation to an operational reality*. In: Maltamo, M., Næsset, E., Vauhkonen, J. (Eds.), *Forestry Applications of Airborne Laser Scanning, Managing Forest Ecosystems*. Springer, Netherlands, pp. 215–240.
- Næsset, E., 2007. Airborne laser scanning as a method in operational forest inventory: status of accuracy assessments accomplished in Scandinavia. *Scand. J. For. Res.* 22, 433–442.
- Næsset, E., 2002. Predicting forest stand characteristics with airborne scanning laser using a practical two-stage procedure and field data. *Remote Sens. Environ.* 80, 88–99. [http://dx.doi.org/10.1016/S0034-4257\(01\)00290-5](http://dx.doi.org/10.1016/S0034-4257(01)00290-5).
- Nilsson, M., 1996. Estimation of tree heights and stand volume using an airborne lidar system. *Remote Sens. Environ.* 56, 1–7. [http://dx.doi.org/10.1016/S0034-4257\(95\)00224-3](http://dx.doi.org/10.1016/S0034-4257(95)00224-3).
- Nurminen, K., Karjalainen, M., Yu, X., Hyypä, J., Honkavaara, E., 2013. Performance of dense digital surface models based on image matching in the estimation of plot-level forest variables. *ISPRS J. Photogramm. Remote Sens.* 83, 104–115. <http://dx.doi.org/10.1016/j.isprsjprs.2013.06.005>.
- Omer, G., Mutanga, O., Abdel-Rahman, E.M., Adam, E., 2015. Performance of support vector machines and artificial neural network for mapping endangered tree species using worldview-2 data in dukuduku forest, South Africa. *IEEE J. Sel. Top. Appl. Earth Obs. Remote Sens.* PP, 1–16. <http://dx.doi.org/10.1109/JSTARS.2015.2461136>.
- Pineiro, G., Perelman, S., Guerschman, J.P., Paruelo, J.M., 2008. How to evaluate models: observed vs. predicted or predicted vs. observed? *Ecol. Model.* 216, 316–322. <http://dx.doi.org/10.1016/j.ecolmodel.2008.05.006>.
- Pitt, D.G., Woods, M., Penner, M., 2014. A comparison of point clouds derived from stereo imagery and airborne laser scanning for the area-based estimation of forest inventory attributes in Boreal Ontario. *Can. J. Remote Sens.* 40, 214–232. <http://dx.doi.org/10.1080/07038992.2014.958420>.
- Polley, H., Schmitz, F., Hennig, P., Kroher, F., 2010. *National forest inventory reports*. In: Tomppo, E., Gschwandter, T., Lawrence, M., McRoberts, R.E. (Eds.), *National Forest Inventories*. Springer, Netherlands, Dordrecht, pp. 223–243 (Chapter 13, Germany).
- Pretzsch, H., 2010. *Forest Dynamics, Growth and Yield*. Springer, Berlin, Heidelberg.
- Rahlf, J., Breidenbach, J., Solberg, S., Næsset, E., Astrup, R., 2014. Comparison of four types of 3D data for timber volume estimation. *Remote Sens. Environ.* 155, 325–333. <http://dx.doi.org/10.1016/j.rse.2014.08.036>.
- R Core Team, 2015. *R: A Language and Environment for Statistical Computing*. R Foundation for Statistical Computing, Vienna, Austria.
- Reese, H., Nilsson, M., Sandström, P., Olson, H., 2002. Applications using estimates of forest parameters derived from satellite and forest inventory data. *Comput. Electron. Agric.* 37, 37–55. [http://dx.doi.org/10.1016/S0168-1699\(02\)00118-7](http://dx.doi.org/10.1016/S0168-1699(02)00118-7).
- Reinartz, P., 2010. The CATENA processing chain-multi-sensor pre-processing: orthorectification, atmospheric correction, future aspects. Presented at the Geoland Forum_6, Toulouse.
- Richter, R., 1996. A spatially adaptive fast atmospheric correction algorithm. *Int. J. Remote Sens.* 17, 1201–1214. <http://dx.doi.org/10.1080/01431169608949077>.
- Richter, R., Schläpfer, D., 2012. *Atmospheric/Topographic Correction for Satellite Imagery (ATCOR-2/3 User Guide)*. German Aerospace Center.
- Richter, R., Schläpfer, D., Müller, A., 2006. An automatic atmospheric correction algorithm for visible/NIR imagery. *Int. J. Remote Sens.* 27, 2077–2085. <http://dx.doi.org/10.1080/01431160500486690>.
- Rouse, J., Haas, R., Schell, J., Deering, D., 1974. Monitoring vegetation systems in the Great Plains with ERTS. In: NASA Special Publication. Presented at the Third EERTS Symposium, pp. 309–317.
- Steinmann, K., Mandallaz, D., Ginzler, C., Lanz, A., 2013. Small area estimations of proportion of forest and timber volume combining Lidar data and stereo aerial images with terrestrial data. *Scand. J. For. Res.* 28, 373–385. <http://dx.doi.org/10.1080/02827581.2012.754936>.
- Stepper, C., Straub, C., Pretzsch, H., 2015a. Using semi-global matching point clouds to estimate growing stock at the plot and stand levels: application for a broadleaf-dominated forest in central Europe. *Can. J. For. Res.* 45, 111–123. <http://dx.doi.org/10.1139/cjfr-2014-0297>.
- Stepper, C., Straub, C., Pretzsch, H., 2015b. Assessing height changes in a highly structured forest using regularly acquired aerial image data. *Forestry* 88, 304–316. <http://dx.doi.org/10.1093/forestry/cpu050>.
- Stoffels, J., Hill, J., Sachtleber, T., Mader, S., Buddenbaum, H., Stern, O., Langshausen, J., Dietz, J., Ontrup, G., 2015. Satellite-based derivation of high-resolution forest information layers for operational forest management. *Forests* 6, 1982–2013. <http://dx.doi.org/10.3390/f6061982>.
- St-Onge, B., Hu, Y., Vega, C., 2008. Mapping the height and above-ground biomass of a mixed forest using lidar and stereo Ikonos images. *Int. J. Remote Sens.* 29, 1277–1294. <http://dx.doi.org/10.1080/01431160701736505>.

- Straub, C., Stepper, C., Seitz, R., Waser, L.T., 2013a. Potential of UltraCamX stereo images for estimating timber volume and basal area at the plot level in mixed European forests. *Can. J. For. Res.* 43, 731–741. <http://dx.doi.org/10.1139/cjfr-2013-0125>.
- Straub, C., Tian, J., Seitz, R., Reinartz, P., 2013b. Assessment of Cartosat-1 and WorldView-2 stereo imagery in combination with a LiDAR-DTM for timber volume estimation in a highly structured forest in Germany. *Forestry* 86, 463–473. <http://dx.doi.org/10.1093/forestry/cpt017>.
- Tomppo, E., Gschwantner, T., Lawrence, M., McRoberts, R.E., 2010. *National Forest Inventories Pathways for Common Reporting*. Springer, Netherlands, Dordrecht.
- Tomppo, E., Olsson, H., Ståhl, G., Nilsson, M., Hagner, O., Katila, M., 2008. Combining national forest inventory field plots and remote sensing data for forest databases. *Remote Sens. Environ.* 112, 1982–1999. <http://dx.doi.org/10.1016/j.rse.2007.03.032>.
- Van Ewijk, K.Y., Randin, C.F., Treitz, P.M., Scott, N.A., 2014. Predicting fine-scale tree species abundance patterns using biotic variables derived from LiDAR and high spatial resolution imagery. *Remote Sens. Environ.* 150, 120–131. <http://dx.doi.org/10.1016/j.rse.2014.04.026>.
- Vanselow, K.A., Samimi, C., 2014. Predictive mapping of dwarf shrub vegetation in an arid high mountain ecosystem using remote sensing and random forests. *Remote Sens.* 6, 6709–6726. <http://dx.doi.org/10.3390/rs6076709>.
- Vastaranta, M., Niemi, M., Wulder, M.A., White, J.C., Nurminen, K., Litkey, P., Honkavaara, E., Holopainen, M., Hyppä, J., 2015. Forest stand age classification using time series of photogrammetrically derived digital surface models. *Scand. J. For. Res.*, 1–37 <http://dx.doi.org/10.1080/02827581.2015.1060256>.
- Vastaranta, M., Wulder, M.A., White, J.C., Pekkarinen, A., Tuominen, S., Ginzler, C., Kankare, V., Holopainen, M., Hyppä, J., Hyppä, H., 2013. Airborne laser scanning and digital stereo imagery measures of forest structure: comparative results and implications to forest mapping and inventory update. *Can. J. Remote Sens.* 39, 382–395. <http://dx.doi.org/10.5589/m13-046>.
- Vauhkonen, J., Maltamo, M., McRoberts, R.E., Næsset, E., 2014. Introduction to forestry applications of airborne laser scanning. In: Maltamo, M., Næsset, E., Vauhkonen, J. (Eds.), *Forestry Applications of Airborne Laser Scanning, Managing Forest Ecosystems*. Springer, Netherlands, pp. 1–16.
- Wang, Z., Ginzler, C., Waser, L.T., 2015. A novel method to assess short-term forest cover changes based on digital surface models from image-based point clouds. *Forestry*. <http://dx.doi.org/10.1093/forestry/cpv012> (cpv012).
- Waser, L.T., Küchler, M., Jütte, K., Stampfer, T., 2014. Evaluating the potential of WorldView-2 data to classify tree species and different levels of ash mortality. *Remote Sens.* 6, 4515–4545. <http://dx.doi.org/10.3390/rs6054515>.
- White, J.C., Wulder, M.A., Varhola, A., Vastaranta, M., Coops, N.C., Cook, B.D., Pitt, D., Woods, M., 2013a. A Best Practices Guide for Generating Forest Inventory Attributes from Airborne Laser Scanning Data using an Area-based Approach (Information Report No. Fl-X-10). Canadian Forest Service, Canadian Wood Fibre Centre, Pacific Forestry Centre, Victoria, BC.
- White, J.C., Wulder, M.A., Vastaranta, M., Coops, N.C., Pitt, D., Woods, M., 2013. The utility of image-based point clouds for forest inventory: a comparison with airborne laser scanning. *Forests* 4, 518–536. <http://dx.doi.org/10.3390/f4030518>.
- Windisch, K., Bronner, G., Mansberger, R., Koukal, T., 2014. Derivation of dominant height and yield class of forest stands by means of airborne remote sensing methods. *Photogramm. Fernerkund. Geoinform.* 2014, 325–338. <http://dx.doi.org/10.1127/1432-8364/2014/0227>.
- Woods, M., Pitt, D., Penner, M., Lim, K., Nesbitt, D., Etheridge, D., Treitz, P., 2011. Operational implementation of a LiDAR inventory in Boreal Ontario. *For. Chronicle* 87, 512–528. <http://dx.doi.org/10.5558/tfc2011-050>.
- Wulder, M.A., Franklin, S.E. (Eds.), 2003. *Remote Sensing of Forest Environments: Concepts and Case Studies*, first ed. Kluwer Academic Publishers, Boston, Dordrecht, London.
- Wulder, M.A., Hall, R.J., Coops, N.C., Franklin, S.E., 2004. High spatial resolution remotely sensed data for ecosystem characterization. *BioScience* 54, 511–521.
- Wulder, M.A., White, J.C., Nelson, R.F., Næsset, E., Ørka, H.O., Coops, N.C., Hilker, T., Bater, C.W., Gobakken, T., 2012. Lidar sampling for large-area forest characterization: a review. *Remote Sens. Environ.* 121, 196–209. <http://dx.doi.org/10.1016/j.rse.2012.02.001>.
- Zlinszky, A., Heilmeier, H., Balzter, H., Czucz, B., Pfeifer, N., 2015. Remote sensing and GIS for habitat quality monitoring: new approaches and future research. *Remote Sens.* 7, 7987–7994. <http://dx.doi.org/10.3390/rs70607987>.